

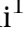



pRB immunostaining in the differential diagnosis between pleomorphic xanthoastrocytoma and glioblastoma with giant cells

Valeria Barresi,¹  Michele Simbolo,¹  Chiara Ciaparrone,¹ Serena Pedron,¹ Andrea Mafficini¹  & Aldo Scarpa^{1,2} 

¹Department of Diagnostics and Public Health, University of Verona, and ²ARC-NET Research Centre, University and Hospital Trust of Verona, Verona, Italy

Date of submission 25 June 2022

Accepted for publication 5 August 2022

Published online Article Accepted 9 August 2022

Barresi V, Simbolo M, Ciaparrone C, Pedron S, Mafficini A & Scarpa A

(2022) *Histopathology* 81, 661–669. <https://doi.org/10.1111/his.14768>

pRB immunostaining in the differential diagnosis between pleomorphic xanthoastrocytoma and glioblastoma with giant cells

Aims: Pleomorphic xanthoastrocytoma (PXA) is a rare circumscribed glioma, characterized by frequent *BRAF* p. V600E mutation, and classified as grade 2 or 3. Owing to overlapping clinical–pathological features, the histological distinction from glioblastoma (GBM) with giant cells (GCs) is challenging. Based on the high frequency of *TP53* and *RBI* alterations in the latter, this study aimed to assess the value of *BRAF*, p53, and pRB immunostainings in the differential diagnosis.

Methods and results: In 37 GBMs with $\geq 30\%$ GCs and in eight PXAs, we assessed the alterations of 409 cancer-related genes and immunostainings for *BRAF*, p53, and pRB. GBMs with GCs were *TP53*-mutated in 30 cases, *RBI*-altered in 11, and *BRAF*-mutated in none. PXAs were *BRAF*-mutated in six cases, *TP53*-mutated in three, and *RBI*-altered in

none. pRB immunostaining was lost in 25 GBMs (11 *RBI*-altered and 14 *RBI*-unaltered), retained in all PXAs and six GBMs, and inconclusive in six GBMs. pRB loss had 100% specificity and 80.6% sensitivity for GBM with GCs. P53 immunostaining was observed in 22 *TP53*-mutated GBMs and in one *TP53*-mutated PXA. It showed 87.5% specificity and 60% sensitivity to identify GBM with GCs. *BRAF* immunostaining corresponded to *BRAF* mutation status and it had 100% specificity and 75% sensitivity for detecting PXA.

Conclusion: This study shows for the first time that loss of pRB immunostaining is sensitive and specific for distinguishing GBM with GCs from PXA in routine practice. Thus, it could complement an immunohistochemical panel that includes *BRAF* and p53 immunostainings for the differential diagnosis.

Keywords: giant cell, glioblastoma, pleomorphic xanthoastrocytoma, pRB, *RBI*

Introduction

Pleomorphic xanthoastrocytoma (PXA) is a rare circumscribed astrocytic glioma¹ that is mainly localized to the temporal lobe^{2,3} and affects children and young adults.³ It is histologically characterized by a

mixture of pleomorphic (often multinucleated and sometimes lipidized), epithelioid, or spindle cells, frequent eosinophilic granular bodies and lymphocytic infiltration, and genetically by recurrent *BRAF* p. V600E mutation (76.1%) and *CDKN2A* homozygous deletion (84%).³ Based on the mitotic count, it is classified as grade 2 or grade 3.¹

Owing to its histological features, PXA should be distinguished from several other tumours, including giant-cell glioblastoma (GBM).¹ This is a subtype of

Address for correspondence: V Barresi, Department of Pathology and Public Health, Policlinico G.B. Rossi, P.le L.A. Scuro, 10, 37134, Verona, Italy. e-mail: valeria.barresi@univr.it

GBM that features a gross circumscription, and is histologically characterized by multinucleated giant cells in a background of small, often fusiform cells, and lymphocytic infiltrate.⁴ The molecular landscape of giant-cell GBM is dominated by impairment of the *TP53/MDM2* and *PTEN/PI3K* pathways.⁵ Thus, strong and diffuse p53 immunostaining favours giant-cell GBM in the differential diagnosis of PXA.⁶ Nonetheless, not all *TP53* mutations result in p53 immunohistochemical overexpression,⁷ and PXAs may rarely harbour *TP53* mutations.⁸

We recently found that, above the high frequency of *TP53* mutations, GBMs histologically featuring at least 30% giant cells (GCs) display a significantly higher rate (25.6%) of *RB1* alterations than conventional GBMs (9.4%).⁵ This finding, also reported by other authors,⁹ suggests that the alteration of *RB1* could be a further distinctive feature of GBMs with GCs.

The immunohistochemical loss of the retinoblastoma protein (pRB), which is encoded by *RB1*, represents a good surrogate for detecting *RB1* alterations.¹⁰ Although pRB immunostaining was previously assessed in GBMs,^{10,11} it was not specifically analysed in the subgroup of GBMs with GCs or in PXAs.

In this study we aimed to assess and compare the accuracy of pRB, p53, and BRAF p. V600E immunostainings in the differential diagnosis between GBM with at least 30% GCs and PXA, in a series of 45 cases genetically characterized using next-generation sequencing (NGS).

Materials and methods

CASES

All PXAs diagnosed in our unit were revised by one pathologist (V.B.) and the eight cases with a confirmed diagnosis were included in this study.

Thirty-two (cases 1GL, 5GL, 9GL, 42GL–71GL) GBMs with GCs previously analysed in other studies^{5,12} and an additional five cases were also considered.

A pathologist (V.B.) revised the histological slides of all cases, to assess the presence of eosinophilic granular bodies (EGB), lymphocytic infiltrate, and spindle cells to establish the histological grade of PXA according to the criteria of the 5th edition of the World Health Organization (WHO) classification of central nervous system (CNS) tumours,¹³ and to quantify the percentage of GCs in GBMs.⁵ A representative paraffin block was selected for the immunohistochemical, fluorescence *in situ* hybridisation (FISH) and molecular (in cases 1X to 14X) analyses.

Data on the tumour localization and patients' overall survival (OS) were retrieved using the clinical records.

ETHICS

This study was approved by the Local Ethics Committee of AOUI Verona (protocol no. 35628, 2020/06/29).

MOLECULAR AND COPY NUMBER VARIATION STATUS OF CANCER-RELATED GENES

In 32 GBMs with GCs (cases 1GL, 5GL, 9GL, and 42GL–71GL), we had already assessed tumour mutational burden (TMB), mutations, and copy number variations (CNV) of 409 cancer-related genes using the targeted NGS panel OncoPrint Tumour Mutational Load (TML) (Thermo Fisher, Waltham, MA, USA), which covers 1.65 Mb of genomic space.^{5,12} In a subset of cases (42GL–71GL), the results were confirmed using the SureSelectXT HS CD Glasgow Cancer Core assay (Agilent Technologies, Santa Clara, CA, USA).⁵

In the remaining five GBMs with GCs and eight PXAs (cases 1X–14X), we used the OncoPrint Tumour Mutational Load (TML) panel (Thermo Fisher) to assess the mutations and CNV of 409 cancer-related genes.

In brief, DNA was obtained from 10 formalin-fixed paraffin-embedded (FFPE) consecutive 4- μ m sections of a representative paraffin block using the QIAamp DNA FFPE Tissue Kit (Qiagen, Hilden, Germany) and qualified as previously reported.¹⁴ Sequencing was performed on the Ion Torrent platform using 20 ng of DNA for each multiplex polymerase chain reaction (PCR) amplification and subsequent library construction. The quality of the libraries was evaluated using the Agilent 2100 Bioanalyzer on-chip electrophoresis (Agilent Technologies). Libraries were clonally amplified by emulsion PCR with the Ion OneTouch OT2 System (Thermo Fisher) and sequencing was performed on Ion Proton (Thermo Fisher) loaded with Ion PI Chip v3. Torrent Suite Software v.5.10 (Thermo Fisher) was used for data analysis, including alignment to the hg19 human reference genome and variant calling. The filtered variants were annotated using a custom pipeline based on vcfib (<https://github.com/ekg/vcfib>), SnpSift,¹⁵ Variant Effect Predictor (VEP),¹⁶ and the NCBI RefSeq database. Additionally, alignments were visually verified with the Integrative Genomics Viewer (IGV) v.2.9¹⁷ to confirm the presence of identified mutations. Germline mutations were assigned based on the method described Sun *et al.*¹⁸

CNVs were evaluated using OncoCNV v.6.8,¹⁹ comparing the BAM files obtained from tumour samples with those obtained from blood samples of four healthy males. The software includes a multifactor normalization and annotation technique that enables the detection of large copy number changes from amplicon sequencing data and permits the visualisation of the output per chromosome.

FLUORESCENCE IN SITU HYBRIDISATION (FISH)

All cases were additionally tested for CNV of *CDKN2A* using FISH and LSI *CDKN2A/CEP 9* Probes (Vysis/Abbott, Molecular Europe, Wiesbaden, Germany), according to the manufacturer's instructions. Slides were examined using an Olympus (Tokyo, Japan) BX61 fluorescence microscope equipped with a 100× oil immersion objective and a triple bandpass filter for simultaneous detection of Spectrum Orange, Spectrum Green, and DAPI signals. Two hundred nonoverlapping nuclei containing a minimum of two reference probes (CEP 9 probe) signals were counted. Cases with two green signals (control probe on chromosome 9 centromeres) and no orange signals (reference probe on *CDKN2A* locus) in at least 30% of the cells were considered to have *CDKN2A* homozygous deletion.

IMMUNOHISTOCHEMISTRY

All samples were immunostained using antibodies against RB gene protein (pRB) (clone 13A10, Leica Biosystems, Newcastle, UK; dilution 1:150), p53 (clone DO-7, Leica Biosystems; 1:50) and BRAF (clone VE1, Roche Diagnostics, Indianapolis, IN, USA; prediluted).

pRB immuno-expression was classified as “lost” when the neoplastic cells were negative and the non-neoplastic cells (internal positive control) were positive, “retained” when both the neoplastic and non-neoplastic cells were positive, and “inconclusive” when both the neoplastic and non-neoplastic cells were negative.

p53 immuno-expression was considered positive in cases showing strong staining in at least 10% of neoplastic cells.^{20,21}

BRAF staining was classified as positive only in cases with unequivocal cytoplasmic. *BRAF* p.V600E mutated melanoma was used as a positive control.

STATISTICAL ANALYSIS

Given the limited number of PXAs in this cohort, we performed a preliminary analysis to assess the power to detect different pRB staining between these and GBMs with GCs. Considering previous data, we

estimated that ~50% GBMs with GCs could feature pRB loss due to either gene alterations⁵ or promoter methylation.²² As a recent NGS analysis of 23 PXAs reported no *RB1* alterations,⁸ we approximated that pRB loss could range from 0% to 10% in these tumours. Under these hypotheses, the statistical power to detect a difference in pRB expression ranged from 95% (if real PXA loss = 0%) to 51% (if real PXA loss = 10%). We applied Fisher's exact test to analyse whether histopathological (EGBs, lymphocytic infiltrate, or spindle cell morphology), immunohistochemical (pRB1, p53, and BRAF p. V600E immunostainings) or genetic (*CDKN2A* homozygous deletion) features were significantly different between GBMs with GCs and PXA. The Mann–Whitney test was applied to evaluate the differences in TMB counts and age of onset in these two subgroups.

To estimate the diagnostic value of pRB–, p53+, and BRAF p. V600E+ immunostainings in the differential diagnosis between GBM with GCs and PXA, we calculated their sensitivity [true positive/(true positive+false negative)] and specificity [true negative/(true negative+false positive)] for GBM with GCs or PXA and assessed their accuracy using the area under the receiver operating characteristic (ROC) curve (AUC).

Finally, we applied the Mantel–Cox log-rank test to assess the strength of association between tumour type (GBM with GCs versus PXA) and overall survival (OS). OS was assessed using the Kaplan–Meier method, using the date of surgery as the entry data and length of survival until the patient's death as the endpoint. Patients who died of independent diseases were censored.

Statistical significance was set at $P < 0.05$. Analyses were performed using MedCalc for Windows version 15.6 (MedCalc Software, Ostend, Belgium).

Results

EOSINOPHILIC GRANULAR BODIES (EGBS), BUT NOT LYMPHOCYTIC INFILTRATE OR SPINDLE CELL MORPHOLOGY, WERE DISTINCTIVE TO PXA

The clinical–pathological, molecular, and immunohistochemical findings are summarized in Figure 1. The age of onset was significantly lower for PXAs (mean: 35 ± 22 years; age range: 16–68 years) than for GBMs with GCs (mean: 52 ± 16.5 years; age range: 15–78 years) ($P = 0.04$). Half of PXAs (4/8) and most GBMs with GCs (17/34 cases) were localized in the temporal lobe.

Five PXAs were classified as grade 2 and three as grade 3. EGBs were found in 7/8 PXAs (87.5%), but

in no GBMs with GCs ($P < 0.0001$). Lymphocytic infiltrate and spindle cell morphology characterized all, or almost all (7/8), PXAs and most (27/37 and 25/37) GBMs with GCs ($P = 0.168$; $P = 0.404$, respectively).

All the patients with PXA remained alive at a follow-up of 14–67 months, while 20 patients with GBMs (54%) died during the follow-up period of 8–79 months. The OS length was significantly longer in patients with PXA ($P = 0.008$).

RB1 ALTERATIONS WERE SPECIFIC TO GBM WITH GIANT CELLS

The genetic alterations of cases 42GL–71GL, 1GL, 5GL and 9GL were detailed in previous studies.^{5,12} Details of the mutations of 409 cancer-related genes in cases 1X–14X are reported in Table S1.

All GBMs and PXAs were *IDH1/2* wildtype.

Thirty GBMs with GCs (81%) and three PXAs (37.5%) featured *TP53* mutations (Figure 1). GBMs with GCs had frequent *PTEN* (13/37; 35%) and *RB1* (11/37; 30%) alterations, while these genes were unaltered in all PXAs. A subset of GC-GBMs, but not PXAs, had MMR genes and *ATRX* mutations, or *EGFR* amplification (seven, five, and five cases, respectively). Most PXAs (6/8; 75%), but not GC-GBMs, had *BRAF* p. V600E mutation, which co-occurred with *CDKN2A* homozygous deletion in four cases (50%) and with *CDKN2A* hemizygous deletion in one.

CDKN2A copy number variations were confirmed using FISH analysis. *CDKN2A* homozygous deletion had similar frequency in PXAs and GBMs with GCs ($P = 0.226$).

CONCURRENT GAINS OF CHROMOSOME 7 AND LOSS OF CHROMOSOME 10 WERE SPECIFIC TO GBM WITH GCS

The status of chromosome arms was inferred based on the chromosomal position of each gene.

Twelve (37%) GBMs with GCs, but no PXAs, had concurrent loss of chromosome 10 and gains of chromosome 7.

None of the cases harboured loss of the entirety of chromosome 13.

TUMOUR MUTATIONAL BURDEN (TMB) WAS HIGHER IN GBM WITH GCS THAN IN PXA

TMB counts ranged between 0.9 and 219.8 muts/Mb (mean: 19.2 ± 41.6 ; median 8.75) in GBMs with

GCs and between 0.8 and 2.7 muts/Mb (mean: 2.4 ± 1.2 ; median: 2.61) in PXAs ($P = 0.0001$). Thirteen GBMs with GCs, but no PXAs, were hypermutated (TMB ≥ 10 muts/Mb).

PRB IMMUNOHISTOCHEMISTRY SHOWED HIGH SPECIFICITY IN DISTINGUISHING PXA

pRB staining could be assessed in 31 GBMs with GCs (the remaining six cases had inconclusive staining) and in all eight PXAs.

pRb loss was found in most GBMs with GCs (25/31, 80.6%) but in no PXAs (100%) ($P = 0.0001$) (Figure 2) (specificity: 100%; sensitivity: 80.6%; AUC: 0.903, $P < 0.0001$) (Table 1).

P53 staining was positive (diffusely and strongly in the majority of tumour cells) in 22/37 (60%) GBMs with GCs, but in only one (12.5%) PXA ($P = 0.021$) (Figure 2) (specificity: 87.5%; sensitivity: 60%; AUC: 0.735, $P = 0.0017$) (Table 1).

BRAF p. V600E staining was positive in all six *BRAF* mutated PXAs and negative in all GBMs with GCs ($P < 0.0001$) (Figure 2) (specificity: 100%; sensitivity: 75%; AUC: 0.875, $P < 0.0001$) (Table 1).

PRB IMMUNOHISTOCHEMICAL LOSS WAS FOUND ALSO IN RB1 UNALTERED GBMS WITH GCS

Of the 25 GBMs with pRB loss, 11 displayed *RB1* alterations (homozygous or hemizygous deletion coupled with the truncating mutation of the other allele) (Figure 1), four (cases 46GL, 51GL, 56GL, 58GL) had *RB1* variants of unknown significance (details in Table S2), and 10 did not show any *RB1* alterations detectable using NGS.

All GBMs with GCs and the PXA with p53 immunohistochemical positivity had *TP53* mutations, but eight GBMs with GCs and two PXAs with *TP53* mutations were negative for p53.

All PXAs *BRAF* p. V600E positive at immunohistochemistry had *BRAF* p.V600E mutation.

Discussion

PXA and GBM with GCs share several clinical and pathological features, including preferential localisation in the temporal lobes,^{1,2,4} age at onset in young adults,^{3,23} and the histological presence of multinucleated, pleomorphic and spindle cells, and lymphocytic infiltrates.^{3,4} These overlapping aspects may result in difficulties in the differential diagnosis. However, PXA has a better prognosis (5-year overall

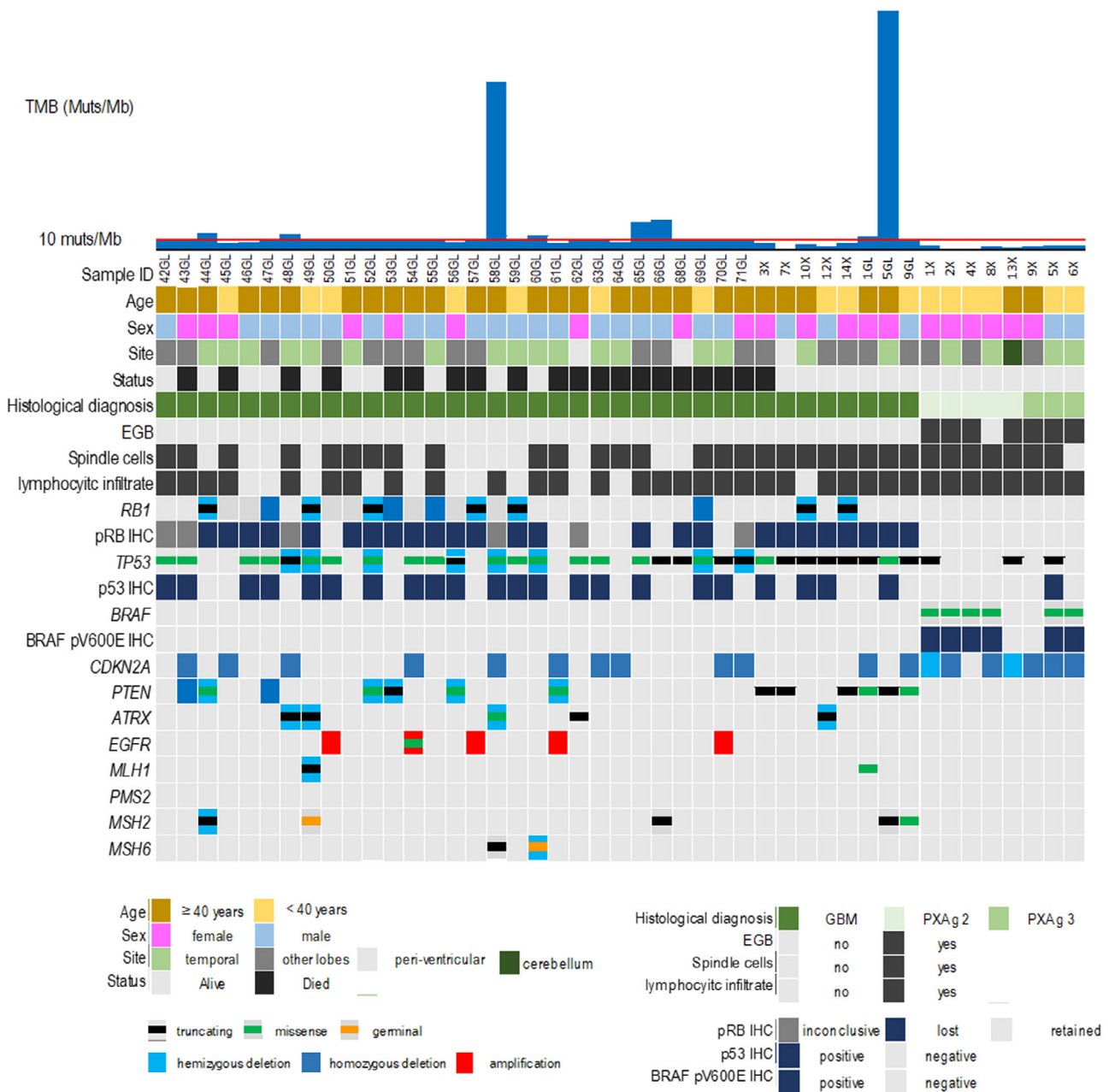


Figure 1. Clinical-pathological features, gene alterations, and immuno-expression of pRB, p53, and BRAF p.V600E in 37 GBMs with GCs and 8 PXA. Samples are sorted by ID number and histological diagnosis. EGB, eosinophilic granular bodies.

survival: 80.8% for PXA grade 2 and 47.6% for grade 3³) than giant-cell GBM (5-year overall survival: 12.3%²³) and grade 2 tumours may be cured with total resection and without additional chemoradiotherapy.²⁴ Therefore, distinctive histological, immunohistochemical, or molecular aspects, which may aid in the differential diagnosis, are desired for the proper treatments of patients.

The assessment of the DNA methylation profile has proven to be a reliable method for the classification of CNS tumours.²⁵ A recent study showed that 40 of 220 tumours classified as PXA according to the methylation profile had been histologically diagnosed as GBM,²⁶ emphasizing the challenges of the differential diagnosis between these two entities. Although methylation analysis could be of significant help in

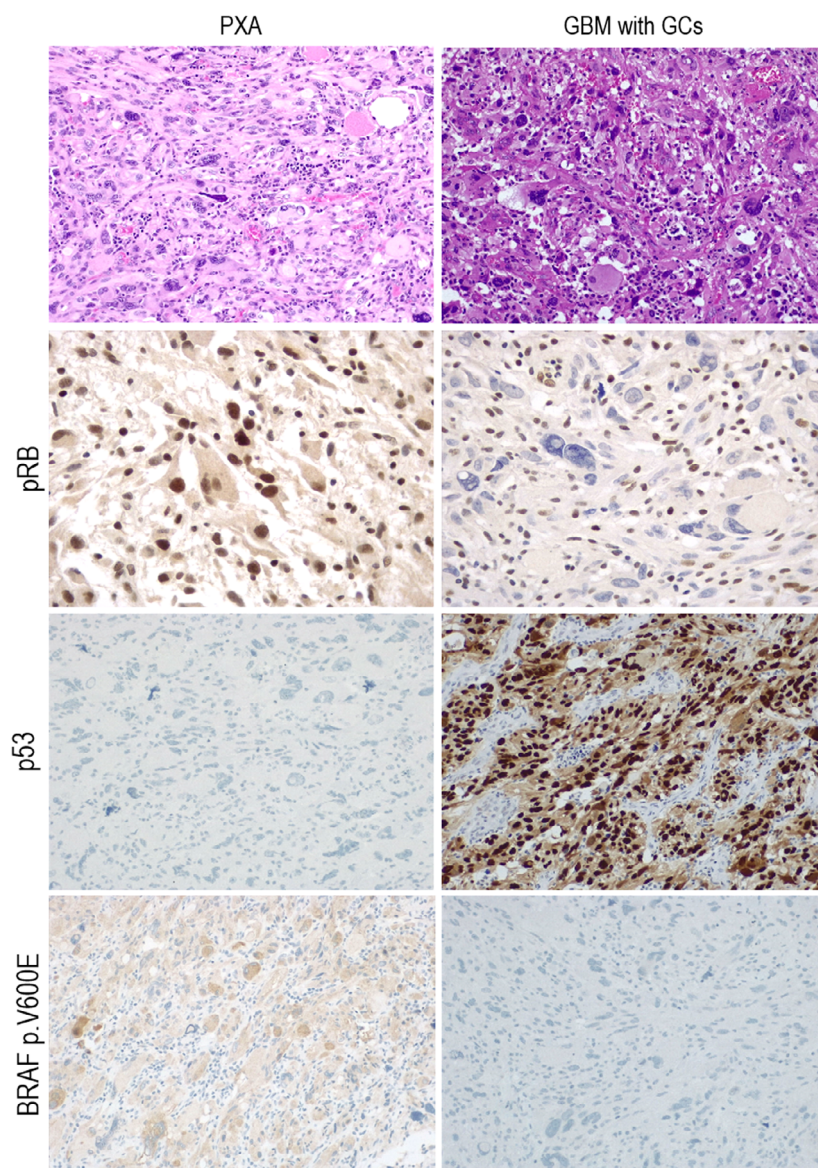


Figure 2. Different immunostainings for pRB, p53, and BRAF p. V600E in PXA and GBM with GCs. PXA retains nuclear pRB immunostaining, is negative (<10% stained cells) for p53, and shows cytoplasmic staining for BRAF p. V600E. GBM with GCs is negative for pRB, shows p53 staining, and lacks BRAF p. V600E staining. H&E: $\times 200$ magnification; pRB: $\times 400$ magnification; p53: $\times 200$ magnification; BRAF p. V600E: $\times 200$ magnification.

distinguishing between PXA and GBM for clinical purposes, this does not give conclusive results in a proportion of cases,²⁶ and the need for sophisticated instruments and specialized personnel makes it difficult to access this technology in many centres. Due to the unavailability in our lab, it was not carried out in this study.

Herein, we confirmed that GBM with GCs and PXA share a preferential localisation in the temporal lobe; although age at diagnosis partially overlapped, GBM with GCs affected older subjects.

EGBs were exclusive to PXAs and represented a useful distinctive aspect, while lymphocytic infiltrate and spindle cell morphology were common to both entities.

BRAF p. V600E mutation was found only in PXAs and, in accordance with previous evidence,^{1,3} it represented the most frequent (75%) genetic alteration in these tumours, co-occurring with *CDKN2A* homozygous deletion in most cases. Notably, there was a perfect agreement between NGS and immunohistochemistry, as BRAF-positive immunostaining was restricted to the mutated cases. In accordance with previous studies,^{27–29} we did not detect *BRAF* mutations or BRAF p. V600E immunostaining in GC-GBMs. Therefore, BRAF immunohistochemical positivity is an accurate diagnostic marker, with 75% sensitivity and 100% specificity for PXA.

TP53 mutations were found in the majority (81%) of GBMs with GCs and in three (37.5%) PXAs.

Table 1. Sensitivity, specificity, and area under receiver operating characteristic (ROC) curve for the detection of GBM with GCs of pRB, p53, and BRAF p. V600E immunostainings in the differential diagnosis versus PXA

Immunostaining	Sensitivity (%)	Specificity (%)	AUC
pRB–	80.6	100	0.903
p53+	60	87.5	0.735
BRAF p.V600E+*	75	100	0.875

*Specificity, sensitivity, and AUC for PXA.

However, this resulted in p53 immunohistochemical overexpression in only 22 (60%) of the former and in one (12.75%) of the latter. Thus, p53-positive immunostaining was 60% sensitive and 85% specific for GBM with GCs in the differential diagnosis of PXA in our series.

Based on the assumption that GBMs histologically featuring at least 30% GCs are enriched in *RB1* alterations,⁵ we analysed for the first time the possible diagnostic value of pRB immunohistochemistry in the distinction between GBM with GCs and PXA. pRB immuno-expression was lost in 25 GBMs with GCs, but only 15 of these (60%) were *RB1*-altered at NGS. This apparent discrepancy might be due to other *RB1* inactivation mechanisms, such as promoter hypermethylation, which was previously demonstrated in GBMs featuring pRB immunohistochemical loss in the absence of *RB1* mutations or deletions.²² In accordance with a previous study that did not demonstrate *RB1* alterations in 23 PXAs analysed using NGS,⁸ all PXAs in our series were *RB1* wildtype and retained pRB immunohistochemical expression. Thus, pRB immunohistochemical loss was 80.6% sensitive and 100% specific to GBM with GCs. The loss of pRB immunostaining had a higher diagnostic accuracy than p53 overexpression in distinguishing GBM with GCs from PXA, as demonstrated by the AUC values. However, pRB immunostaining was inconclusive in six (16%) GBMs with GCs that showed negative neoplastic and non-neoplastic cells even upon repeated assays. Since all cases with inconclusive staining were dated more than 8 years, pRB immunostaining is likely influenced by technical issues.

Recently, DNA methylation profiling identified a new type of circumscribed high-grade glioma, named high-grade glioma with pleomorphic and pseudopapillary features (HPAP).³⁰ This features *RB1* alterations in a frequency of 26%, pleomorphic multinucleated giant cells in some cases, and characteristic entire loss of chromosome 13,³⁰ which was not observed in any tumours of the present series.

CDKN2A homozygous deletion did not differ between GBMs with GCs and PXA, whereas *PTEN* alterations were frequent in the former and absent in the latter. In accordance with a previous study,³ none of the PXA harboured co-occurring gains of chromosome 7 and loss of chromosome 10, which is considered a molecular hallmark of GBM,⁴ whereas this was present in 37% of GBMs with GCs.

This study was the first to assess TMB in PXAs and demonstrated a low rate of mutations/Mb, and no hypermutated cases. This represented a further distinctive feature from GBMs with GCs, which displayed higher TMB counts and hypermutated cases.^{9,12,28}

In conclusion, this study demonstrates for the first time that the immunohistochemical loss of pRB is highly sensitive and 100% specific to GBM with GCs in the differential diagnosis with PXA. If verified in larger, multicentric, cohorts, pRB immunostaining could complement an immunohistochemical panel including p53 and BRAF immunostainings to distinguish these tumours in routine practice. The introduction of pRB immunohistochemistry may be cost-effective in labs that should optimize this staining. However, this could be useful for an early distinction between PXA and GBM with GCs prior to obtaining molecular results or could further substantiate the differential diagnosis when molecular tests are not available.

The findings of this study also showed that NGS might underestimate the percentage of *RB1* alteration in GBMs with GCs and that the proportion of cases with silencing of this gene might be higher than expected.

Acknowledgement

Open Access Funding provided by Universita degli Studi di Verona within the CRUI-CARE Agreement.

Funding information

This study was supported by the University of Verona, Italy (FUR 2020 to VB).

Author contributions

VB conceptualized the study, collected the cases, performed the histological review and the statistical analyses, interpreted the data and drafted the article.

MS, CC, SP, and AM performed formal analyses and interpreted the data and edited the article. AS interpreted the data and reviewed the article.

Conflict of interest

None to declare.

Data availability statement

Data will be available upon reasonable request to the corresponding author.

References

- Giannini C, Capper D, Figarella-Branger D *et al.* Pleomorphic xanthoastrocytoma. In Brat DJ, Ellison DW, Figarella-Branger D *et al.* eds. *WHO classification of tumours editorial board. Central nervous system tumours*. Lyon: International Agency for Research on Cancer, 2021.
- Rodrigues A, Bhambhani H, Medress ZA, Malhotra S, Hayden-Gephart M. Differences in treatment patterns and overall survival between grade II and anaplastic pleomorphic xanthoastrocytomas. *J. Neurooncol.* 2021; **153**: 321–330.
- Vaubel R, Zschemack V, Tran QT *et al.* Biology and grading of pleomorphic xanthoastrocytoma-what have we learned about it? *Brain Pathol.* 2021; **31**: 20–32.
- Louis DN, Aldape KD, Capper D *et al.* Glioblastoma, idh-wildtype. In Brat DJ, Ellison DW, Figarella-Branger D *et al.* eds. *WHO classification of tumours editorial board. Central nervous system tumours*. Lyon: International Agency for Research on Cancer, 2021.
- Barresi V, Simbolo M, Mafficini A *et al.* Idh-wild type glioblastomas featuring at least 30% giant cells are characterized by frequent *rb1* and *nf1* alterations and hypermutation. *Acta Neuropathol. Commun.* 2021; **9**: 200.
- Martinez-Diaz H, Kleinschmidt-DeMasters BK, Powell SZ, Yachnis AT. Giant cell glioblastoma and pleomorphic xanthoastrocytoma show different immunohistochemical profiles for class iii neuronal antigens and p53 but share reactivity for class iii beta-tubulin. *Arch. Pathol. Lab. Med.* 2003; **127**: 1187–1191.
- Yemelyanova A, Vang R, Kshirsagar M *et al.* Immunohistochemical staining patterns of p53 can serve as a surrogate marker for tp53 mutations in ovarian carcinoma: an immunohistochemical and nucleotide sequencing analysis. *Mod. Pathol.* 2011; **24**: 1248–1253.
- Phillips JJ, Gong H, Chen K *et al.* The genetic landscape of anaplastic pleomorphic xanthoastrocytoma. *Brain Pathol.* 2019; **29**: 85–96.
- Cantero D, Mollejo M, Sepulveda JM *et al.* Tp53, *atrx* alterations, and low tumor mutation load feature idh-wildtype giant cell glioblastoma despite exceptional ultra-mutated tumors. *Neurooncol. Adv.* 2020; **2**: vdz059.
- Goldhoff P, Clarke J, Smirnov I *et al.* Clinical stratification of glioblastoma based on alterations in retinoblastoma tumor suppressor protein (*rb1*) and association with the proneural subtype. *J. Neuropathol. Exp. Neurol.* 2012; **71**: 83–89.
- Suwala AK, Stichel D, Schrimpf D *et al.* Glioblastomas with primitive neuronal component harbor a distinct methylation and copy-number profile with inactivation of *tp53*, *pten*, and *rb1*. *Acta Neuropathol.* 2021; **142**: 179–189.
- Barresi V, Simbolo M, Mafficini A *et al.* Ultra-mutation in idh wild-type glioblastomas of patients younger than 55 years is associated with defective mismatch repair, microsatellite instability, and giant cell enrichment. *Cancers (Basel)* 2019; **11**: 1279.
- Louis DN, Ohgaki H, Wisteler OD *et al.* *Who classification of tumors of the central nervous system*. Lyon: IARC, 2016.
- Simbolo M, Gottardi M, Corbo V *et al.* DNA qualification workflow for next generation sequencing of histopathological samples. *PLoS One* 2013; **8**: e62692.
- Cingolani P, Patel VM, Coon M *et al.* Using drosophila melanogaster as a model for genotoxic chemical mutational studies with a new program, snpsift. *Front. Genet.* 2012; **3**: 35.
- McLaren W, Pritchard B, Rios D, Chen Y, Flicek P, Cunningham F. Deriving the consequences of genomic variants with the ensembl api and snp effect predictor. *Bioinformatics* 2010; **26**: 2069–2070.
- Robinson JT, Thorvaldsdottir H, Winckler W *et al.* Integrative genomics viewer. *Nat. Biotechnol.* 2011; **29**: 24–26.
- Sun JX, He Y, Sanford E *et al.* A computational approach to distinguish somatic vs. germline origin of genomic alterations from deep sequencing of cancer specimens without a matched normal. *PLoS Comput. Biol.* 2018; **14**: e1005965.
- Boeva V, Popova T, Lienard M *et al.* Multi-factor data normalization enables the detection of copy number aberrations in amplicon sequencing data. *Bioinformatics* 2014; **30**: 3443–3450.
- Ammendola S, Caldonazzi N, Simbolo M *et al.* H3k27me3 immunostaining is diagnostic and prognostic in diffuse gliomas with oligodendroglial or mixed oligoastrocytic morphology. *Virchows Arch.* 2021; **479**: 987–996.
- Takami H, Yoshida A, Fukushima S *et al.* Revisiting TP53Mutations and immunohistochemistry-a comparative study in 157 diffuse gliomas. *Brain Pathol.* 2015; **25**: 256–265.
- Nakamura M, Yonekawa Y, Kleihues P, Ohgaki H. Promoter hypermethylation of the *rb1* gene in glioblastomas. *Lab. Invest.* 2001; **81**: 77–82.
- Kozak KR, Moody JS. Giant cell glioblastoma: a glioblastoma subtype with distinct epidemiology and superior prognosis. *Neuro Oncol.* 2009; **11**: 833–841.
- Ida CM, Rodriguez FJ, Burger PC *et al.* Pleomorphic xanthoastrocytoma: natural history and long-term follow-up. *Brain Pathol.* 2015; **25**: 575–586.
- Capper D, Stichel D, Sahm F *et al.* Practical implementation of DNA methylation and copy-number-based CNS tumor diagnostics: the Heidelberg experience. *Acta Neuropathol.* 2018; **136**: 181–210.
- Ebrahimi A, Korshunov A, Reifenberger G *et al.* Pleomorphic xanthoastrocytoma is a heterogeneous entity with *ptert* mutations prognosticating shorter survival. *Acta Neuropathol. Commun.* 2022; **10**: 5.
- Gerstung M, Papaemmanuil E, Campbell PJ. Subclonal variant calling with multiple samples and prior knowledge. *Bioinformatics* 2014; **30**: 1198–1204.
- Shi ZF, Li KK, Kwan JSH *et al.* Whole-exome sequencing revealed mutational profiles of giant cell glioblastomas. *Brain Pathol.* 2019; **29**: 782–792.
- Tosuner Z, Gecer MO, Hatiboglu MA, Abdallah A, Turna S. *Braf* v600e mutation and *brf1* immunoprotein profiles in different types of glioblastoma. *Oncol. Lett.* 2018; **16**: 2402–2408.
- Pratt D, Abdullaev Z, Papanicolau-Sengos A *et al.* High-grade glioma with pleomorphic and pseudopapillary features (hpap): a proposed type of circumscribed glioma in adults harboring

frequent tp53 mutations and recurrent monosomy 13. *Acta Neuropathol.* 2022; **143**: 403–414.

Supporting Information

Additional Supporting Information may be found in the online version of this article:

Table S1: List of somatic and germline mutations identified in samples 1X to 14X.

Table S2: RB1 variants of unknown significance found in four GBMs with GCs and RB1 immunohistochemical loss.